Solid State Compounds with Tin−Tin Bonding. $Yb_{36}Sn_{23}$: A Novel Compound Containing Oligomeric Tin Anions

E. Alejandro Leon-Escamilla and John D. Corbett*

Department of Chemistry and Ames Laboratory—DOE,[1] Iowa State University, Ames, Iowa 50011

Received July 22, 1998

Reaction of appropriate amounts of the elements in Ta at 1100 °C leads to formation of the title phase in high yield. Hydrogen impurities in small amounts do not obscure its formation. $Yb_{36}Sn_{23}$ crystallizes in tetragonal space group *P*4/*mbm* (No. 127) with $a = 12.3869(5)$ Å, $c = 22.935(1)$ Å, $Z = 2$. The structure features a linear tin hexamer, five dimers, and seven isolated tin atoms per formula unit. These proportions lead to a closed-shell oxidation state count for simple octet assignments $(Yb^{+2})_{36}(Sn_6^{-14})(Sn_2^{-6})_5(Sn^{-4})_7$ and a Zintl phase classification. Dimensionally, all cations appear to be Yb^{II}. The hexamer of tin atoms has as its genesis the close contact of Sn atoms that center confacial square antiprismatic arrangements of Yb atoms (closely related to the parent W_5Si_3 structure). These interconnect with elongated square prisms in a 6:1 proportion to generate the $n =$ six member of Parthé's homologous series $A_{5n+6}B_{3n+5}$. Electrical conductivity measurements as a function of temperature show that the compound is a poor metal ($\rho_{298} \approx 130\ \mu\Omega$·cm). The latter property is not uncommon for compounds containing clusters of the early p elements.

Introduction

Exploration of the *anionic* chemistry of the post-transition main-group (p) elements has been delightful and rewarding in the variety of novel clusters and networks that can be found in their compounds with the active metals.[2] The great majority of these are also valence compounds (Zintl phases) in modern bonding terms, or close to this limit. Among these systems, the tendency of tin to form classical octet-rule homoatomic polyanions has been particularly remarkable. These have included condensed pentagonal-faced dodecahedra in K_8Sn_{25}, a defect clathrate-I structure in K_8Sn_{44}, etc.,[3] a tunnel structure in $NaGaSn_2$[4] in which the anionic network is isoelectronic with gray tin, a complex 3D network in Na_5Sn_{13},[5] an intergrowth structure containing dimeric and linear pentameric tin oligomers in $Ca_{31}Sn_{20}$,[6] and zigzag chains built of interconnected square planar (and in this case, hyperelectronic) Sn_5^{-14} units in $Ca_{6.2}Mg_{3.8}Sn_7$.[7]

The discovery of another example, the novel binary phase $Yb_{36}Sn_{23}$, resulted from our continuing interest in the effects of hydrogen on the family of 5:3 compounds comprising the alkaline-earth (Ae = Ca, Sr, or Ba) and divalent rare-earth-metal (R = Sm, Eu, Yb) pnictides (Pn = As, Sb, Bi) and tetrelides (Tt = Si, Ge, Sn, Pb).[8] We have in the course of this demonstrated that adventitious hydrogen can generate numerous very stable ternary $(Ae,R)_5(Pn,Tt)_3H$ compounds and thereby obscure the existence of truly binary phases. For instance, the discovery of several members of the $(Ae,R)_{16}Pn_{11}$ ($Ca_{16}Sb_{11}$-type) family[9] as well as the existence of certain Mn_5Si_3-type examples had been precluded by the presence of very stable hydrides with the orthorhombic Ca_5Sb_3F (formerly β-Yb_5Sb_3)-type structure.[10] Comparable effects have also been demonstrated in tetrelide systems, such that several reported Ae_5Tt_3 phases with Cr_5B_3-type structures are actually ternary hydrides (stuffed Cr_5B_3- or La_5Pb_3O-type).[8,11]

It was our examination of the specific Yb−Sn system around the composition Yb_5Sb_3 that led to the discovery of $Yb_{36}Sn_{23}$. A previous report of both Mn_5Si_3- and Cr_5B_3-type phases at this composition[12] originated with impurities and could not be reproduced in the clean binary system. We describe here the synthetic studies, a single-crystal X-ray structure determination, and some electrical and magnetic property measurements on the new $Yb_{36}Sn_{23}$ with its novel mixture of monomeric, dimeric, and hexameric tin anions. These yield a formulation that is consistent with Zintl phase concepts.[2] The compound is also the first $n =$ six member of structural series $A_{5n+6}B_{3n+5}$[13] originating from W_5Si_3-type slabs.[14] We have earlier reported on the $n = 2$ and 5 members of this series, $Ca_{16}Sb_{11}$[9] and $Ca_{31}Sn_{20}6$ ($Pu_{31}Pt_{20}$-type[15]), respectively.

Experimental Section

Synthesis. All materials were handled in low-humidity gloveboxes (<0.1 ppm H_2O) filled with He or N_2 and following standard techniques.[6,9,10] The elements were loaded into Ta tubes that were

(1) This research was supported by the Office of the Basic Energy Sciences, Materials Sciences Division, U.S. Department of Energy. The Ames Laboratory is operated for DOE by Iowa State University under Contract No. W-7405-Eng-82.

(2) Corbett, J. D. In *Chemistry, Structure and Bonding of Zintl Phases and Ions*; Kauzlarich, S. M., Ed.; VCH: New York, 1996; Chapter 3.
(3) Zhao, J.-T.; Corbett, J. D. *Inorg. Chem.* **1994**, *33*, 5721.
(4) Vaughey, J. T.; Corbett, J. D. *J. Am. Chem. Soc.* **1996**, *118*, 12098.
(5) Vaughey, J. T.; Corbett, J. D. *Inorg. Chem.* **1997**, *36*, 4316.
(6) Ganguli, A. K.; Guloy, A. M.; Leon-Escamilla, E. A.; Corbett, J. D. *Inorg. Chem.* **1993**, *32*, 4349.
(7) Ganguli, A. K.; Corbett, J. D.; Köckering, M. *J. Am. Chem. Soc.* **1998**, *120*, 1223.
(8) Leon-Escamilla, E. A. Ph.D. Dissertation, Iowa State University, 1996.
(9) Leon-Escamilla, E. A.; Hurng, W.-M.; Peterson, E. S.; Corbett, J. D. *Inorg. Chem.* **1997**, *36*, 703.
(10) (a) Leon-Escamilla, E. A.; Corbett, J. D. *J. Alloys Compd.* **1994**, *206*, L15. (b) Leon-Escamilla, E. A.; Corbett, J. D. *J. Alloys Compd.* **1998**, *265*, 104.
(11) Leon-Escamilla, E. A.; Corbett, J. D. to be published.
(12) Palenzola, A.; Cirafici, S. *J. Phase Equilib.* **1991**, *12*, 482 and references therein.
(13) Leroy, J.; Moreau, J.; Paccard, D.; Parthé, E. *J. Less-Common Met.* **1980**, *76*, 131.
(14) Aronsson, B. *Acta Chem. Scand.* **1955**, *9*, 1107.
(15) Cromer, D. T.; Larson, A. C. *Acta Crystallogr.* **1977**, *33B*, 2620.

10.1021/ic980861x CCC: $18.00
Published on Web 01/27/1999

Table 1. Selected Crystallographic Data and Refinement Parameters for $Yb_{36}Sn_{23}$

fw	8959.31
space group, Z	$P4/mbm$ (No. 127), 2
lattice params[a]	
a (Å)	12.3869(5)
c (Å)	22.935(1)
vol (Å^3)	3519.0(3)
density, calcd (g/cm^3)	8.455
abs. coeff (cm^{-1}, Mo Kα)	551.9
R/R_w[b] (%)	3.1/3.6

[a] Lattice parameters calculated from Guinier powder pattern data, λ = 1.540 562 Å, 23 °C. [b] $R = \Sigma||F_o| - |F_c||/\Sigma|F_o|$; $R_w = [\Sigma w(|F_o| - |F_c|)^2/\Sigma w(F_o)^2]^{1/2}$; $w = \sigma_F^{-2}$.

subsequently arc-welded shut under Ar and jacketed in fused silica containers. The silica containers were in these cases connected to a high-vacuum line in order to run high-temperature reactions under continuous vacuum to ensure the absence of hydrogen, Ta being permeable to hydrogen above about 550 °C.[16] Products containing $Yb_{36}Sn_{23}$ in high yield (>90%, as subsequently estimated on the basis of a calculated Guinier powder pattern) were obtained on reaction of the appropriate mixture of Yb (99.99%, Ames Lab.) and Sn (99.999%, Aesar). Higher yields of the title phase were obtained for compositions slightly richer in Yb, i.e., 5Yb + 3Sn (62.5 rather than the theoretical 61.0 atom % Yb), probably because of Yb metal losses through volatility. The reactants were generally held under vacuum at 1150 °C for 2−4 h and then slowly cooled (10 °C/h) to 650 °C. Conversely, only slightly lower yields of the title phase were obtained when the high-quality Yb metal was used as provided and the silica jackets were sealed off before heating. In this case, dehydration of the silica contributes a hydrogen source as well.[17] These low hydrogen concentrations did not appear to interfere with the formation of $Yb_{36}Sn_{23}$; however, small amounts of impurity phases (<3−5%) might have been missed in the relatively complex powder pattern of the target phase. On the other hand, reactions loaded with excess hydrogen, viz., $Yb_5Sn_3H_4$ ($2YbH_2 + 3Yb + 3Sn$), yielded 10−15% of a $Yb_5Sn_3H_x$ phase with the stuffed Cr_5B_3-type structure.[8]

Powder X-ray Diffraction. Powder patterns were obtained from small ground samples held between cellophane tape. An Enraf-Nonius Guinier camera, Cu Kα1 radiation (λ = 1.540 56 Å), and Si (NIST) as an internal standard were employed. The Guinier patterns were digitized with an LS20 line scanner (KEJ Instruments, Stockholm, Sweden) and standardized according to the Si line positions with the program SCANPI8.[18] Lattice parameters of the sample were then calculated by least-squares of indexed 2θ data. There is considerable resemblance of the experimental pattern of $Yb_{36}Sn_{23}$ to those of related $Pt_{31}Pu_{20}$-type phases $Ca_{31}Sn_{20}$, $Sr_{31}Pb_{20}$, and $Yb_{31}Pb_{20}$, appropriate to their structural similarities.

Single-Crystal Structure Study. A black platelike crystal 0.23 × 0.18 × 0.10 mm was mounted in a glass capillary inside the glovebox and checked for singularity through Laue photographs. One quadrant of diffraction data ($2\theta_{max}$ = 50°) was collected at room temperature on an Enraf-Nonius CAD4 automatic diffractometer with Mo Kα radiation according to the tetragonal cell determined from indexing of 25 centered reflections. Some details of the data collection and refinement are listed in Table 1. The diffraction data were corrected for Lorentz polarization effects and for adsorption empirically with the aid of three ψ-scans. Later, a more thorough absorption correction (μ = 551.9 cm^{-1}) by DIFABS[19] was applied before anisotropic refinement, and this yielded generally smaller thermal ellipsoids.

On the basis of the systematic absences, the space groups $P4bm$ (No. 100), $P4b2$ (117), and $P4/mbm$ (127) were possible. Only the last space group provided a model with good statistics from a direct methods approach (SHELX86),[20] and this contained the correct positions of all atoms. The structure subsequently was refined with the aid of the TEXSAN package.[21] The final cycle of full-matrix least-squares refinement with 1205 observed reflections ($I > 3\sigma_I$) and 88 variables (all positional and anisotropic thermal parameters) converged at $R(F)/R_w$ = 0.031/0.036. No significant deviation from full atom occupancies was evident. Table 2 gives the atomic positional and isotropic-equivalent thermal parameters, and Table 3 lists important interatomic distances in the structure. More crystallographic and refinement data as well as the anisotropic displacement parameters are contained in the Supporting Information, and the F_o/F_c listing along with the other information is available from J.D.C.

Table 2. Refined Positional Parameters of and Isotropic-Equivalent Ellipsoids for $Yb_{36}Sn_{23}$

atom	Wyckoff position	x	y	z	B_{eq} (Å^2)[a]
Sn1	2a	0	0	0	1.0(1)
Sn2	4e	0	0	0.1663(1)	0.53(7)
Sn3	4e	0	0	0.3018(1)	0.44(6)
Sn4	4e	0	0	0.4336(1)	0.50(6)
Sn5	4g	0.0884(2)	$x + 1/2$	0	0.66(7)
Sn6	4h	0.1569(2)	$x + 1/2$	1/2	0.65(7)
Sn7	8k	0.1641(1)	$x + 1/2$	0.2156(1)	0.78(5)
Sn8	8k	0.3059(1)	$x + 1/2$	0.1308(1)	0.55(5)
Sn9	8k	0.3484(1)	$x + 1/2$	0.3595(1)	0.67(5)
Yb1	4f	0	1/2	0.12807(9)	0.78(4)
Yb2	4f	0	1/2	0.2789(1)	0.74(4)
Yb3	4f	0	1/2	0.4293(1)	0.71(4)
Yb4	4g	0.3330(1)	$x + 1/2$	0	1.12(5)
Yb5	8j	0.0824(1)	0.2199(1)	1/2	0.80(6)
Yb6	16l	0.41239(8)	0.28485(9)	0.36815(5)	0.76(4)
Yb7	16l	0.07601(8)	0.21237(9)	0.23792(4)	0.61(4)
Yb8	16l	0.05618(8)	0.79001(9)	0.09202(4)	0.73(4)

[a] $B_{eq} = (8\pi^2/3)\sum_i\sum_j U_{ij} a_i^* \vec{a}_j \vec{a}_{ij}$.

Properties. Electrical resistivity data were measured at 35 MHz over 150−300 K by the electrodeless "Q" method[22] with the aid of a Hewlett-Packard 4342A Q Meter. For this purpose, approximately 100 mg of powdered sample with an average grain diameter of 500 μm was dispersed with nearly eight times as much chromatographic Al_2O_3 and sealed under He in a Pyrex tube. Magnetic susceptibility measurements were made on two different preparations. These were held between two silica rods within a close-fitting silica tube and were measured under He at 3 T over the range 6−300 K on a Quantum Design MPMS SQUID magnetometer. The raw data were corrected for susceptibilities of the container and the ion cores.

Results and Discussion

Syntheses. The most recent Yb−Sn phase diagram report by Palenzola and Cirafici[12] indicates that both hexagonal Mn_5Si_3-type and tetragonal Cr_5B_3-type phases exist near 62.5 atom % Yb, the latter being observed above 1090 °C. Neighboring phases are Yb_5Sn_4 (55.5 atom % Yb) and Yb_2Sn (66.7 atom % Yb) with the Gd_5Si_4 and Ni_2In structure types, respectively. Our findings in this system (see Experimental Section) are that $Yb_{36}Sn_{23}$ (61.0 atom % Yb) forms in high yield on cooling samples in the composition range 60.8−62.5 atom % Yb from 1150 °C. Hydrogen in low concentrations, either purposely loaded as YbH_2 or as an inadvertent impurity, does not obscure the formation of $Yb_{36}Sn_{23}$. This was demonstrated by parallel reactions carried out under dynamic vacuum (to remove hydrogen) or in sealed containers in the presence of low concentrations of hydrogen. On the other hand, reactions with excess hydrogen lead to a ternary Yb_5Sn_3H product with a stuffed Cr_5B_3-type

(16) Imoto, H.; Corbett, J. D. *Inorg. Chem.* **1981**, *20*, 145.
(17) Rustad, D. S.; Gregory, N. W. *Inorg. Chem.* **1982**, *21*, 2929.
(18) Werner, P.-E. *SCANPI8*, version 8; Arrhenius Laboratory, Stockholm University: Stockholm, Sweden, 1990.
(19) Walker, N.; Stuart, D. *Acta Crystallogr.* **1983**, *A39*, 159.
(20) Sheldrick, G. M. SHELXS-86; Universität Göttingen: Göttingen, Germany, 1986.
(21) *TEXSAN*, version 6.0; Molecular Structure Corp.: The Woodlands, TX, 1990.
(22) Shinar, J.; Dehner, B.; Beaudry, B. J.; Peterson, D. T. *Phys. Rev* **1988**, *37B*, 2066.

Table 3. Interatomic Distances (<4.5 Å) in $Yb_{36}Sn_{23}$

atom−atom		*d* (Å)	atom−atom		*d* (Å)
Sn1−Sn2	(×2)	3.814(3)	Yb3−Sn6	(×2)	3.190(3)
Yb8	(×8)	3.421(1)	Sn9	(×2)	3.100(3)
Sn2−Sn3		3.107(5)	Yb2		3.451(2)
Yb7	(×4)	3.241(2)	Yb3		3.242(4)
Yb8	(×4)	3.186(2)	Yb5	(×4)	3.963(2)
Sn3−Sn2		3.107(5)	Yb6	(×4)	3.949(1)
Sn4		3.023(5)	Yb4−Sn5	(×2)	3.310(3)
Yb6	(×4)	3.256(2)	Sn5		4.285(4)
Yb7	(×4)	3.154(2)	Sn8	(×2)	3.037(2)
Sn4−Sn3		3.023(5)	Yb8	(×4)	3.797(1)
Sn4		3.046(7)	Yb8	(×4)	4.062(2)
Yb5	(×4)	3.283(2)	Yb5−Sn4	(×2)	3.283(2)
Yb6	(×4)	3.245(2)	Sn6		3.323(4)
Sn5−Sn5		3.098(7)	Sn6		3.334(2)
Yb1	(×2)	3.321(2)	Sn9	(×2)	3.695(2)
Yb4	(×2)	3.310(3)	Yb3		3.963(2)
Yb4		4.285(4)	Yb5		3.464(3)
Yb8	(×4)	3.294(2)	Yb6	(×2)	3.685(1)
Sn6−Yb3	(×2)	3.190(3)	Yb6	(×2)	3.812(1)
Yb5	(×2)	3.323(4)	Yb6−Sn3		3.256(2)
Yb5	(×2)	3.334(2)	Sn4		3.245(2)
Yb6	(×4)	3.520(1)	Sn6		3.520(1)
Sn7−Sn8		3.156(3)	Sn7		3.921(2)
Yb1		3.506(3)	Sn9		3.331(2)
Yb2		3.219(3)	Sn9		3.397(1)
Yb6	(×2)	3.921(2)	Yb3		3.949(1)
Yb7	(×2)	3.315(2)	Yb5		3.685(1)
Yb7	(×2)	3.384(1)	Yb5		3.812(1)
Yb8	(×2)	3.501(2)	Yb6		3.455(2)
Sn8−Sn7		3.156(3)	Yb6	(×2)	4.070(2)
Yb1		3.401(2)	Yb7		3.610(1)
Yb4		3.037(2)	Yb7		3.779(1)
Yb7	(×2)	3.086(2)	Yb7−Sn2		3.241(2)
Yb8	(×2)	3.224(2)	Sn3		3.154(2)
Yb8	(×2)	3.437(2)	Sn7		3.315(2)
Sn9−Yb2		3.236(3)	Sn7		3.384(1)
Yb3		3.100(3)	Sn8		3.086(2)
Yb5	(×2)	3.695(2)	Sn9		3.391(2)
Yb6	(×2)	3.331(2)	Yb2		3.803(1)
Yb6	(×2)	3.397(1)	Yb6		3.610(1)
Yb7	(×2)	3.391(2)	Yb6		3.779(1)
Yb1−Sn5	(×2)	3.321(2)	Yb7		3.707(2)
Sn7	(×2)	3.506(3)	Yb7	(×2)	3.951(2)
Sn8	(×2)	3.401(2)	Yb8		3.726(1)
Yb2		3.459(3)	Yb8−Sn1		3.421(1)
Yb8	(×4)	3.751(1)	Sn2		3.186(2)
Yb2−Sn7	(×2)	3.219(3)	Sn5		3.294(2)
Sn9	(×2)	3.236(3)	Sn7		3.501(2)
Yb1		3.459(3)	Sn8		3.224(2)
Yb3		3.451(2)	Sn8		3.437(2)
Yb7	(×4)	3.803(1)	Yb1		3.751(1)
			Yb4		3.797(1)
			Yb4		4.062(2)
			Yb7		3.610(1)
			Yb8	(×2)	3.808(2)

structure, a phase previously misidentified as Yb_5Sn_3. We also believe that their Yb_5Sn_4 is a hydride.[8] Because of the large amount of data, our studies on the effects of hydrogen on the alkaline-earth and divalent rare-earth-metal tetrelides and details on these so-called A_5Tt_3 "binaries" will be the subject of a later manuscript.[11] The earlier observation of a Mn_5Si_3-type structure as well in the binary system[12] must have originated from a Yb_5Sn_3Z phase because of substantial impurities, Z = C, N, O, ...[23] We have been unable to obtain such a structure type in either of the Yb_5Sn_3 or Yb_5Sn_3H systems, although they do occur for Sm and Yb tetrel hydride systems.

Structure of $Yb_{36}Sn_{23}$. This novel phase crystallizes in a primitive tetragonal cell, *P*4/*mbm*, with 17 independent atom positions, nine Sn and eight Yb, and exhibits as its main features a remarkable linear tin hexamer, five tin dimers, and seven isolated tin atoms dispersed among Yb atoms in the independent unit ($Z = 2$). Figures1 and 2 are [001] and [100] views of the cell, respectively, with tin drawn as smaller solid spheres. The heavy lines between the Sn atoms denote short contacts, presumably bonds. The $Yb_{36}Sn_{23}$ structure can be considered the n = six member of Parthé's homologous series, $A_{5n+6}B_{3n+5}$.[13] This series exhibits an infinite array of B atoms (Sn here) that center confacial antiprisms and square prisms of A (Yb) atoms that are joined along the *z* direction in a 6:1 sequence. Each square antiprism forms part of a slab that can be related to the W_5Si_3-type parent structure ($n = \infty$). Large distortions of the parent structure are observed closer to where the single slab containing square prismatic $A_{8/2}B$ units is intergrown with the others. (The W_5Si_3-type structure consists of two polyhedral fragments, square antiprisms built of W1 and centered by Si that form confacial chains along 0,0,*z* and $^1/_2,^1/_2,z$, and parallel chains of tetrahedral $[(Si2)_4W2]$ units that share Si edges along $0,^1/_2,z$, etc. The latter silicon atoms also bridge shared antiprism edges on two chains of the first type (see Figure 3a). Nearly all compounds that crystallize in the W_5Si_3 structure show short M−M contacts between the atoms in the W2 position $(0,^1/_2,^1/_4)$.)

Reminiscent of $Ca_{31}Sn_{20}$ ($n = 5$),[6] which contains a linear pentamer in a related structure, the independent half of the $Yb_{36}Sn_{23}$ structure can be described in terms of four slab sections centered at $z \approx 0.43$, 0.30, 0.17, and 0. The first section at $z \approx 0.43$ depicted in Figure 3a is essentially that of W_5Si_3, and it is mirrored by an identical slab centered at $z \simeq 0.57$. This contains square antiprisms built of Yb5 and Yb6 atoms that are centered by Sn4 atoms at 0,0,0.43 and $^1/_2,^1/_2$,0.43 and interconnected by isolated edge-bridging Sn6 and Sn9 atoms bonded to adjacent square antiprisms. (Sn4 is one of the central pair in the Sn_6 unit along this channel, as can be followed with the aid of Figure 4a.) The Sn6 and Sn9 atoms are also members of the edge-sharing tetrahedra that surround the Yb3 atoms along $0,^1/_2,z$. The second section at $z \approx 0.30$ (not depicted) is nearly equivalent to the first, but the squares of Yb6 and Yb7 atoms constituting the antiprisms have twisted a little and are now centered by Sn3 in the hexamer. The third section at $z \approx 0.17$, Figure 3b, shows the related network around the Sn2 atoms that lie at the ends of the hexamer. Here, the squares of Yb7 and Yb8 have twisted anew, and Sn7 and Sn8 that bridge their edges have now formed dimers by opening the shared edges of the nominal tetrahedra. This section is still related to the W_5Si_3-type structure. In the fourth section at 0,0,0, Figure 3c, there are now Yb8 square prisms centered by Sn1 plus in-plane Sn5 dimers, formerly one edge of the tetrahedra along $0,^1/_2,z$, that have displaced into cavities at $0,^1/_2$,0. At this point, the principal features of the W_5Si_3-type structure have been lost. The oversized square prismatic arrangement is probably the origin of the somewhat larger but fairly spherical thermal ellipsoids found for the Sn1 atom (Table 2). Similar peculiarities were observed for Sn1 in $Ca_{31}Sn_{20}$,[6] and a more extreme situation was found in a square prismatic cavity in $Ca_{16}Sb_{11}$,[9] where disorder of the centering atom was discerned. Despite the distortions in this structure, all self-bonded Sn atoms remain eight-coordinate by Yb, following the general construction motif of the layers, while the isolated Sn6 and Sn9 have 10 Yb neighbors.

The confacial chains of six antiprismatic polyhedra of Yb atoms centered by Sn, with a perpendicular mirror plane at the center, is the origin of the linear hexamer in the structure.

(23) Corbett, J. D.; Garcia, E.; Guloy, A. M.; Hurng, W.-M.; Kwon, Y.-U.; Leon-Escamilla, E. A. *Chem. Mater.* **1998**, *10*, 2824.

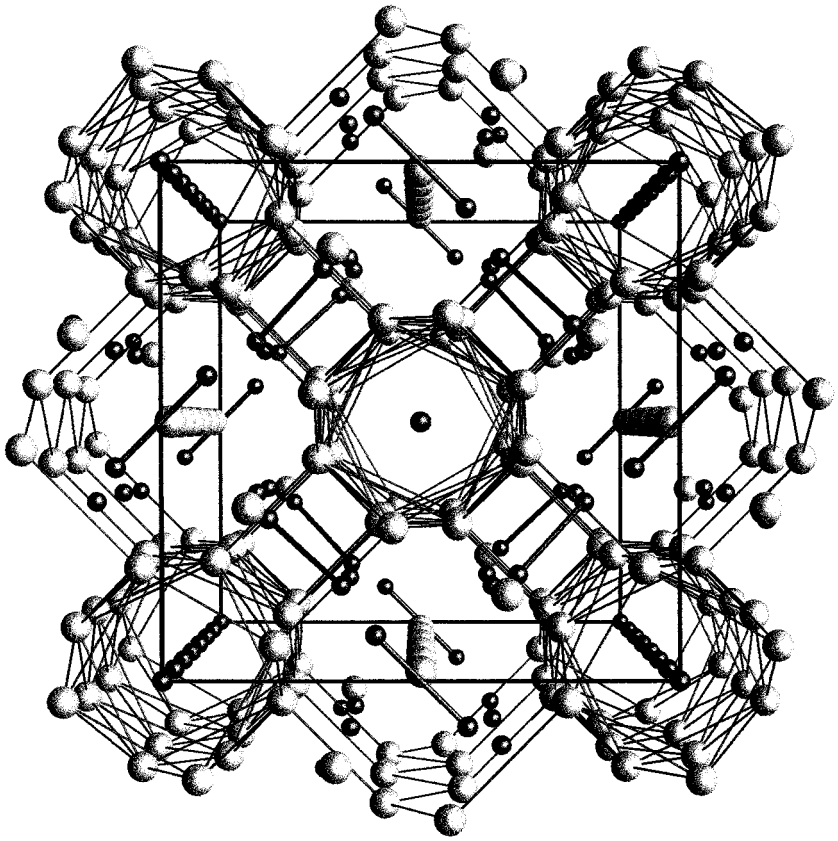

Figure 1. [001] view of the $Yb_{36}Sn_{23}$ structure. Small black and large shaded spheres represent Sn and Yb atoms, respectively. Heavier lines denote Sn−Sn bonds while thin lines between Yb atoms only emphasize geometric features. The main feature is chains of confacial, distorted Yb antiprisms along 0,0,*z* and $^1/_2,^1/_2,z$ that are centered by tin.

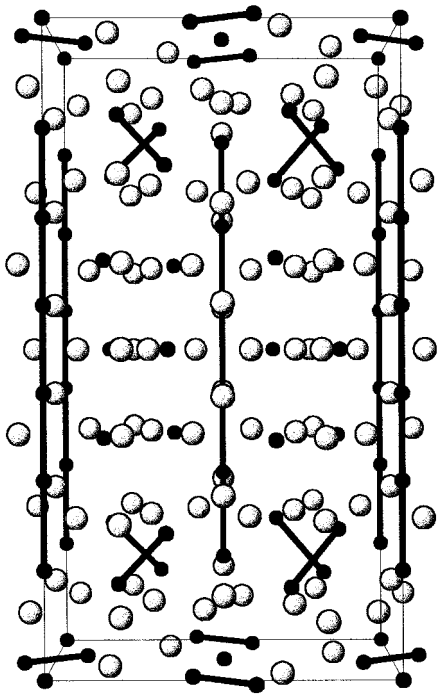

Figure 2. [100] projection of the $Yb_{36}Sn_{23}$ structure, with Sn as the smaller solid spheres. Heavy lines emphasize Sn−Sn bonds.

Interatomic distances in the chain are 3.107(5), 3.023(5), 3.046(7), 3.023, and 3.107 Å for Sn2−Sn3−Sn4−Sn4−Sn3−Sn2, respectively (Figure 4a), while Sn−Sn distances of 3.098(7) and 3.156(3) Å occur in the Sn5−Sn5 and Sn7−Sn8 dimers, respectively. The latter are likewise coordinated by a pair of confacial square antiprisms of Yb. The assumption of formal single bonds between one- and two-bonded tin atoms with distances of 3.02−3.16 Å in $Yb_{36}Sn_{23}$ is in good accord with equivalent interactions in $Ca_{31}Sn_{20}$ (a diamagnetic semiconductor) at 3.06−3.16 Å. Nominal Sn−Sn single bond interactions in other anionic systems include 3.00 Å for the assumed Sn_2^{6-} in Li_7Sn_2,[24] 2.94 Å in SrSn[25] with zigzag chains of 2b-Sn^{-2}, 2.84 Å in the dodecahedral network in K_8Sn_{25}, and 2.81 Å in gray tin.[3] Both charge repulsions within the polytin anions and matrix effects in this tightly packed structure are expected to play important roles in the bond length variations and increased distances in the oligomeric anions. Thus, the longer *d*(Sn7−Sn8) appears to correlate with the fact that both Yb4 and Yb7 are positioned so as to restrict the Sn7−Sn8 approach, the distances between Sn8 and Yb4 and Yb7 being the shortest in the structure. Similarly, the longest Sn2−Sn3 bond is at the end of the hexamer chain where there are fairly short Sn2−Yb8 and Sn3−Yb7 contacts as well as an expectation of a greater charge repulsion from the higher formal charge on 1b-$Sn2^{-3}$.

Additional short Sn−Yb contacts occur between Yb3 and Sn6 and Sn9. These are caused by the constrictive tetrahedral coordination around Yb3 in the slab at $z \approx 0.43$, and its equivalent at $z \approx 0.57$. Both are virtually W_5Si_3-type slabs, and short contacts are generally found between W2 or equivalent atoms that center the edge-sharing tetrahedral chains of Si along $0,^1/_2,z$, etc. Here, the Yb3-centered edge-sharing bitetrahedral unit formed by Sn6 and Sn9 contains a relatively short Yb3−Yb3 contact, 3.242(4) Å, the darker atoms in Figure 4b, while the rest of the Yb−Yb distances in the structure start at 3.45 Å. The meaning

(24) Müller, W. *Z. Naturforsch.* **1974**, *29B*, 304.
(25) Widera, A.; Schäfer, H. *J. Less-Common Met.* **1981**, *77*, 29.

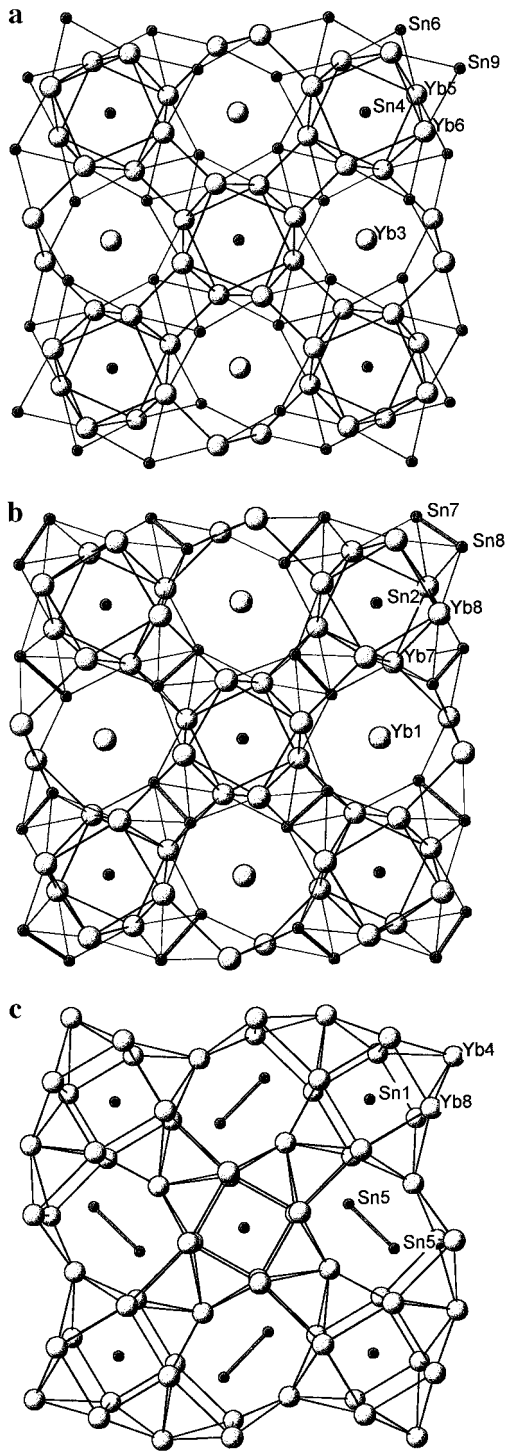

Figure 3. [001] slab sections in $Yb_{36}Sn_{23}$. Small solid and large shaded spheres represent Sn and Yb atoms, respectively, with light lines only to aid perspective. (a) W_5Si_3-like section at $z \approx \pm 0.43$ where Yb5 and Yb6 atoms form the confacial antiprismatic chain centered by Sn4 at 0,0,0.43 etc. and Sn6 and Sn9 atoms centered by Yb3 form the parallel edge-sharing tetrahedral arrangement along $0,{}^1/_2,z$ etc. A second more distorted W_5Si_3-like section at $z \approx \pm 0.30$ is not shown. (b) The distorted slabs around $z \approx \pm 0.17$, showing further twisting of squares in the antiprism of Yb7 and Yb8 that are centered by Sn2, the end member of the Sn_6 unit. Former edge-bridging Sn7 and Sn8 atoms now form dimers. (c) Square prisms centered by Sn1 at $z = 0$ and Sn5−Sn5 dimers in the former tetrahedral columns.

of this closer approach is difficult to judge; it is still 40% greater than twice the Yb crystal radius.[26] Questions about a variation in the oxidation state of this cation (or others) on the basis of

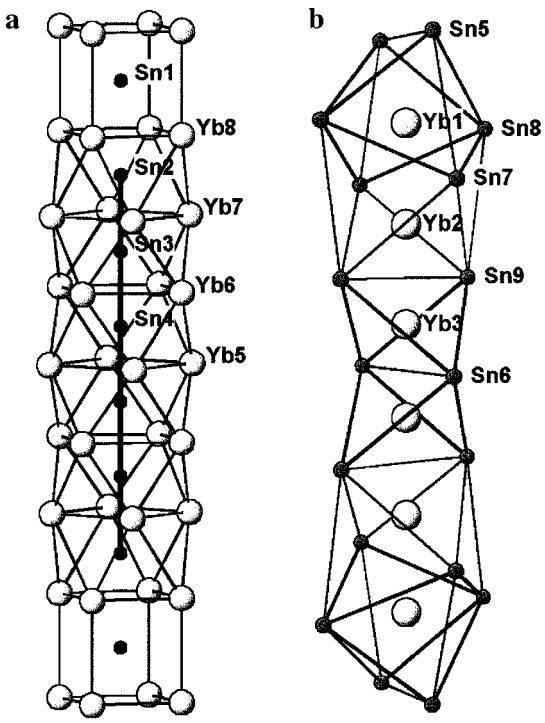

Figure 4. Details of the shared polyhedra in $Yb_{36}Sn_{23}$ viewed from the side ($\bar{c}$ vertical). (a) Sequence of centered square prisms and antiprisms of Yb atoms along $0,0,z$ and ${}^1/_2,{}^1/_2,z$ with a 1:6 proportion. (b) Yb atoms along $0,{}^1/_2,z$, etc. and their Sn coordinations. Heavier lines mark Sn−Sn distances below 5 Å. Yb5 and Sn6 lie on the mirror plane $x,y,{}^1/_2$.

properties (below) cannot be disregarded, although all Yb−Sn distances are quite compatible with the presumed divalency of Yb. The averages sort out well according to just the number of Sn about Yb, 3.14−3.23 Å for four neighbors, 3.26−3.41 Å for those with six contacts. There is nothing akin to the 0.16 Å decrease expected were all the cations in one set of equivalent sites to be entirely Yb^{III}.[26]

Properties. If a classical, localized octet or 8−N scheme is applied here,[2,27] the bonding requirements of tin species match the aggregate for Yb^{II} donors as follows: each hexamer would have a Sn_6^{-14} formulation [four 2b-Sn^{-2} and two 1b-Sn^{-3} (in oxidation states)], while each tin dimer and isolated atom would similarly be described as Sn_2^{-6} and Sn^{-4}, respectively. The 2 hexamers, 10 dimers and 14 isolated tin atoms per cell have an oxidation state sum of −144, and the 72 Yb^{+2} cations in $Yb_{36}Sn_{23}$ ($Z = 2$) make the compound closed shell, that is, a Zintl phase structurally[28] ($36Yb^{+2}$, Sn_6^{-14}, $5Sn_2^{-6}$, $7Sn^{-4}$) and, in principle, semiconducting and diamagnetic. (Of course, the actual charges are not nearly as large as the assigned oxidation states.)

Electrical resistivity measurements as a function of temperature indicate that $Yb_{36}Sn_{23}$ behaves as a poor metal with a room temperature resistivity of 132 $\mu\Omega$·cm and a temperature coefficient of 0.42(4)% K^{-1}. There are two possible explanations of the conductivity results. Certain cation-deficient compounds with W_5Si_3-type structures have been observed to have fractional occupation of the W2 position,[29] and there is a tight polyhedron

(26) Shannon, R. D. *Acta Crystallogr.* **1976**, *A32*, 751.
(27) (a) Schäfer, H.; Eisenmann, B.; Müller, W. *Angew. Chem., Int. Ed. Engl.* **1973**, *12*, 694. (b) Schäfer, H.; Eisenmann, B. *Rev. Inorg. Chem.* **1981**, *3*, 29. (c) Schäfer, H. *Annu. Rev. Mater. Sci.* **1985**, *15*, 1.
(28) Hughbanks, T. *Prog. Solid State Chem.* **1989**, *19*, 329.
(29) Schewe-Miller, I. Ph.D. Dissertation, Universität Stuttgart, Germany, 1990.

about the corresponding Yb3 (above). A small deficiency there would either leave open states on the anions or, more likely, be countered by Yb^{III} elsewhere. Along this line, a range of 0.14% (13.6σ) was observed among the cell volumes refined for five different samples of $Yb_{36}Sn_{23}$. On the other hand, the resistivity is rather low, and another explanation could well apply. Related Cr_5B_3-type Ae_5Tt_3 phases, which appear to be nominal valence compounds as $(Ae^{+2})_5(Tt^{-4})Tt_2^{-6}$ (Ae = Ca−Ba, etc.), are often still metallic. Calculations show the expected, that the π^* states of the dimeric Tt_2^{-6} are the highest lying, and some delocalization of screened electrons therefrom apparently occurs. In fact, a concomitant shortening of the Tt_2 bond is noted on formal oxidation of some of these phases.[8,11] The same could easily apply to Sn_2^{-6} or Sn_6^{-14} in $Yb_{36}Sn_{23}$. Metallic conduction in compounds of this type does not seem so unusual when these involve anionic groups with relatively high formal charges. Many compounds containing polyindium or thallium anion clusters are poor metals even though they are structurally closed shell and diamagnetic,[2] and some phases with anionic polytin networks are semiconductors and diamagnetic.[2−6] In any case, one should not lose sight of the fact that the lower lying electrons in bonds are what determine the interesting architecture in these phases, not the behavior of the least bound electrons.

Magnetic susceptibility measurements on two separate preparations of $Yb_{36}Sn_{23}$ did not afford a lot of information. Both samples appeared to be single phase according to Guinier patterns, but they also had the Yb_5Sn_3 composition used in order to gain a high yield (see Experimental Section). According to the phase diagram,[12] these products should also contain a few percent each of Yb_2Sn + 2Yb impurities. The small magnetism of hcp Yb[30] would probably not be evident, and we assume that the unknown magnetic properties of Yb_2Sn could be responsible for the weak paramagnetism and low moments (0.5−0.9 μ_B) deduced from both by nonlinear fitting to the Curie−Weiss expression.[31] The intrinsic magnetic properties of $Yb_{36}Sn_{23}$ are thus ambiguous, although a Pauli-like term could be buried in the TIP values found. On the other hand, a small proportion of a mixed valency for some Yb could be responsible for the property observations and yet not be evidenced by Yb−Sn distances.

Regardless of the detailed nature of $Yb_{36}Sn_{23}$ and our limited efforts to characterize the properties of this unusual phase, the appearance of this novel result prompts note of how influential very minor changes in cation size or possible electronic effects may be as far as phase stability. The $Yb_{36}Sn_{23}$ structure has not been found for any other combination of alkaline-earth or divalent rare-earth metal with a tetrel element. The Ca−Sn system would have been anticipated to show some resemblance to the Yb−Sn system, since the standard crystal radius of Ca^{2+} is only ca. 1.7% (0.02 Å) smaller than that of divalent Yb^{2+},[26] and the two show parallel chemistries in many pnictide system, e.g., as both A_5Pn_3[10] and $A_{16}Pn_{11}$[9] for A = Ca, Yb with Pn = Sb or Bi. On the other hand, we have found that Ca−Sn reactions at about a 5:3 proportion (and low hydrogen concentrations) lead to the formation of only the other oligomeric structure $Ca_{31}Sn_{20}$. The replacement of Sn by Pb in both Yb and Ca reactions likewise leads to $Yb_{31}Pb_{20}$ and to an incompletely characterized superstructure of a Mn_5Si_3-like compound,[8,32] respectively. This sensitivity of the formation of the present n = six member of Parthé's homologous series to cation size also hints that possible higher members may be attained with careful attention to reaction partner properties.

It is remarkable how novel new phases can still be found in supposedly well-studied binary systems, as for $Yb_{36}Sn_{23}$. Obscuring effects from impurity hydrogen appear to have played an important role in precluding an earlier discovery of this phase. Several compounds with the Cr_5B_3-type structure reported to be formed at approximately the same composition are now known to be hydrides, e.g., Yb_5Sn_3H.[8,11] Hydrogen effects are not unique to this composition; our experimental results strongly suggest that the "binary" Yb_5Sn_4 may be a hydrogen-stabilized compound as well. Additional results from our studies of such polar intermetallic compounds will be the subjects of further reports.[11]

Acknowledgment. We thank J. Ostenson for the magnetic susceptibility measurements.

Supporting Information Available: Tables of additional data collection and refinement information and a listing of the anisotropic displacement parameters. This material is available free of charge via the Internet at http://pubs.acs.org.

IC980861X

(30) Bucher, E.; Schmidt, P. H.; Jayaraman, A.; Andres, K.; Maita, J. P.; Nassau, K.; Dernier, P. D. *Phys. Rev. B* **1970**, *2*, 3911.

(31) Sample 1: TIP = 1.15 × 10^{-2} emu mol^{-1}, θ = −0.7 K, μ_{eff} = 0.49 μ_B. Sample 2: 7.95 × 10^{-3} emu mol^{-1}, 1.1 K, 0.88, respectively. The Curie−Weiss fits were very good.

(32) (a) Helleis, V. O.; Kandler, H.; Leicht, E.; Quiring, W.; Wölfel, E. *Z. Anorg. Allg. Chem.* **1963**, *320*, 86. (b) Guloy, A. M. Ph.D. Dissertation, Iowa State University, 1992.